

# ANALYSIS OF PIEZOCONE DISSIPATION DATA USING DISLOCATION METHODS

By Derek Elsworth,<sup>1</sup> Member, ASCE

**ABSTRACT:** The theory of a moving point dislocation is applied to the rational determination of permeability and consolidation coefficients from piezocone-sounding data. Motion of the process zone in following the penetrometer tip is shown to result in important differences in behavior between static and undrained analogs to penetration. A distinction is drawn between pressure buildup and postarrest dissipation behaviors recorded both at the tip and along the shaft. Tip pressures are shown to become steady within approximately 1 s following drive initiation at a standard rate of 2 cm/s. Shaft pressures within 10 radii of the tip equilibrate within 10 s. Postarrest pressure dissipation at the tip enables consolidation coefficient,  $c$ , to be determined independently. Nonuniqueness in pressure-dissipation response along the shaft is shown to preclude independent determination of consolidation behavior for consolidation coefficients less than about 20 cm<sup>2</sup>/s, under standard penetration. Hydraulic conductivities,  $k$ , are directly evaluated from induced pore pressure magnitudes recorded either at the tip or along the shaft, given a priori knowledge of consolidation coefficient,  $c$ . Piezocone-derived magnitudes of consolidation coefficient enable conductivities to be determined independently of laboratory or material-specific empirical determinations. Relationships are developed for net cone end bearing ( $q_n$ ) as a linear function of elastic parameters and for pore pressure ratio ( $B_q$ ). Pore pressure ratio is shown to be an insensitive index in low  $c$  soils. Results from well-documented field investigations in both normally consolidated and overconsolidated materials are used to independently establish the applicability of the proposed parameter determination techniques. Satisfactory correspondence is obtained.

## INTRODUCTION

Current penetrometer-based methods of determining the permeabilities and consolidation behavior of soils are practically limited to undrained penetration in fine-grained materials. The main factor limiting quantitative evaluation of material parameters in coarser grained soils is the absence of a unified theory to represent the concurrent processes of pore-pressure generation and dissipation in the vicinity of the advancing penetrometer. Instead, qualitative appraisal of soil type represents an established technique in profiling using correlations of depth-corrected cone bearing stress ( $q_n$ ) versus pore pressure ratio ( $B_q$ ) or friction ratio, representing the ratio of sleeve resistance to end bearing resistance [e.g., Sanglerat (1972), Jones and Van Zyl (1981) and Robertson et al. (1986)]. The ability to quantitatively determine the magnitudes of consolidation parameters in situ has been more elusive for the partially drained case. The mechanical model reported by Elsworth (1990, 1991) represents the cone penetration process by a moving volumetric dislocation, as illustrated in Fig. 1. The penetrometer displaces a volume,  $dV$ , under unit advance and may be represented by a point-normal dislocation of equivalent volume. The point dislocation within a saturated porous medium couples displacements with the generation of

<sup>1</sup>Assoc. Prof., Dept. of Mineral Engrg., Pennsylvania State Univ., 104 Mineral Sciences Building, University Park, PA 16802.

Note. Discussion open until March 1, 1994. To extend the closing date one month, a written request must be filed with the ASCE Manager of Journals. The manuscript for this paper was submitted for review and possible publication on February 24, 1992. This paper is part of the *Journal of Geotechnical Engineering*, Vol. 119, No. 10, October, 1993. ©ASCE, ISSN 0733-9410/93/0010-1601/\$1.00 + \$.15 per page. Paper No. 3543.

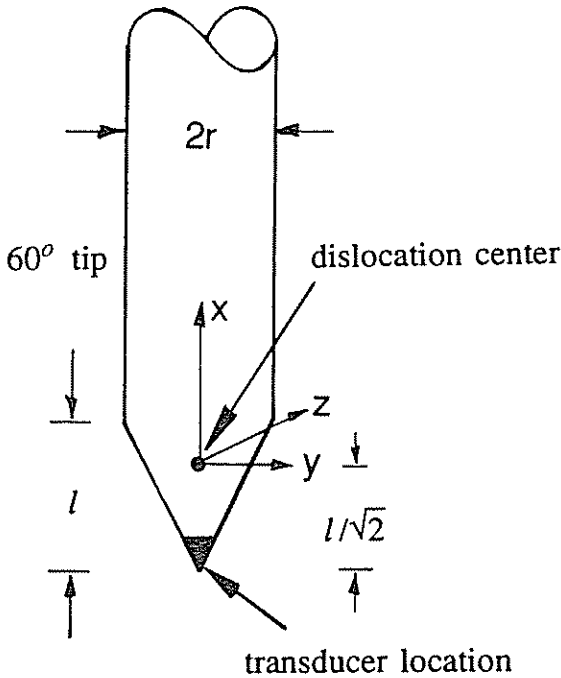


FIG. 1. Geometry of Penetrometer Tip and Point Dislocation

undrained pore pressures within the surrounding medium, and allows for the concurrent dissipation of excess pressures. The moving dislocation is analogous to the penetration process and enables penetration-generated pore pressures to be determined where pressure dissipation occurs concurrently with penetrometer driveage. This model may be conveniently used to define pore-pressure distributions generated in homogeneous and heterogeneous layered materials (Elsworth 1992), and may also be applied in the determination of advective permeabilities of soils (Ylinen and Elsworth 1992). The analogy between a moving dislocation and the penetration process is utilized in the following to define appropriate methods for data reduction in partially drained penetration and to suggest the limits of applicability of these methods.

### SOLUTION VALIDITY

Solution has been previously presented by Elsworth (1990, 1991) to the problem of a point normal dislocation moving within a saturated porous-elastic medium and leaving a remnant linear void. The analogy with cone penetration is clear; however, departure from the true physical system is apparent in that the dislocation is reduced in size to a point, of infinitesimal dimension, and that linear elastic behavior is assumed in the surrounding medium. The applicability of each of these assumptions must be critically examined in order to condition the relevance of the conclusions drawn from the analysis.

### Dislocation Size

Point and line source solutions are known to perform adequately in representing finite features where the location of interest is either reasonably distant from the source or at large magnitudes of elapsed dimensionless time. Since the analysis is for a point dislocation, the results do not differentiate between alternative tip geometries. One approximate method, however, of accounting for the alternative geometries is to consider the coordinate origin to be coincident with the "dilation center" of the penetrometer, as illustrated in Fig. 1. The dilation center is defined as the neutral location behind the cone apex where an incremental advance of the penetrometer will displace an equal amount of material both ahead of and behind that location. The conical volume introduced by cone advance places the dilation center at a distance  $l/\sqrt{2}$ , behind the penetrometer apex where  $l$  = the length of taper. This concept is utilized in the following to differentiate between pressure response at the tip and along the shaft. For a  $60^\circ$  cone, the dilation center is present at a dimensionless distance ( $x/r$ ) of 0.4082 behind the advancing apex, where  $r$  = the radius of the penetrometer and  $x$  is measured from the dilation center as illustrated in Fig. 1.

### Solution Linearity

Perhaps a more severe restriction as to the applicability of the dislocation approach lies within the requirement of elastic response that disregards the presence of both material and geometric nonlinearities in the process zone adjacent to the tip. Behavior is controlled by the material coefficients of modulus of elasticity,  $E$ , Poisson ratios in the drained,  $\nu$ , and undrained states,  $\nu_u$ , and the Skempton (1954) pore pressure parameters  $A$  and  $B$ . Since the material is assumed elastic the deviatoric pore pressure parameter takes the default magnitude of  $A = 1/3$ . A natural paradox exists in our endeavor to determine undisturbed material parameters from any test that, as a natural consequence of the procedure, disturbs soil fabric and properties. Predictions based on the dislocation model are expected to be most applicable where the dimension of the failure process zone surrounding the penetrometer tip is minimized as a result of work hardening type behavior. Less appropriate is application in materials exhibiting elastic-perfectly plastic and strain softening behaviors for which this analysis technique has reduced application. The dislocation concept may be applied equally to materials in both normally consolidated and overconsolidated states, however, the modulus parameters (and parameters dependent on modulus such as consolidation coefficient) that are derived from the data will be representative of the current consolidation condition. If penetration-induced stresses drive the local behavior from an overconsolidated state into virgin behavior, aggregate parameters representing both states of consolidation will be returned.

The applicability of the dislocation analogy to penetration is best gauged in comparing real data with results from the dislocation model.

### APPLICATION OF DISLOCATION ANALYSIS

Results of the dislocation analysis are useful in both devising appropriate data-reduction strategies in the partially drained regime and highlighting the rate dependence of the processes occasioned as a result of penetrometer advance. Penetration rate dependence is apparent in the pore-pressure generation and dissipation response elicited under both undrained and partially

drained states. The following identifies the consequences of practical value that relate to the transient pressure buildup, resulting steady pressure regime, and subsequent transient pressure dissipation response measured in undrained and partially drained piezocone penetration. The findings follow directly from the methods outlined in Elsworth (1991) with all applications relating directly to a standard 60° cone of 10 cm<sup>2</sup> end bearing area.

**Transient Pressure Buildup**

The rate of pore pressure development at the tip is uniquely conditioned by the dimensionless penetration rate  $U_D$  as illustrated in Fig. 2. The magnitudes of the generated dimensionless pore pressures,  $P_D$ , are also dependent on the penetration rate. In the dislocation analysis, a singularity exists at  $x_D = 0$  with the result that both pore pressures at the tip and on the shaft behind show a different spatial dependence. From (12) of Elsworth (1991) the spatial dependencies are

$$P_D x_D = 1 \quad \text{for } x_D \geq 0 \quad \dots \dots \dots (1)$$

and

$$P_D |x_D| = e^{2U_D x_D} \quad \text{for } x_D < 0 \quad \dots \dots \dots (2)$$

where

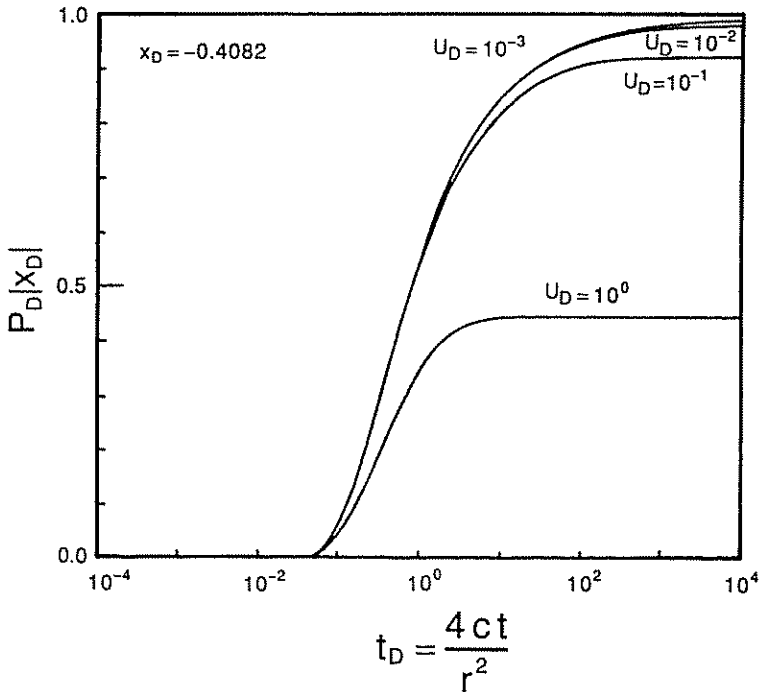


FIG. 2. Transient Generation of Pore Pressures at Tip of Standard 60° Penetrometer

$$P_D = \frac{4(\Delta u) k_i}{Ur \mu} \dots \dots \dots (3)$$

$$U_D = \frac{Ur}{2c} \dots \dots \dots (4)$$

$$x_D = \frac{x}{r} \dots \dots \dots (5)$$

and  $\Delta u$  = induced pore pressure,  $k_i$  = intrinsic permeability,  $\mu$  = dynamic viscosity of the fluid,  $r$  = the radius of the penetrometer,  $U$  = penetration rate, and  $c$  = isotropic coefficient of consolidation (i.e.,  $C_h = C_v$ ). All notation is defined in Appendix II.

For a 60° cone,  $x_D = -0.4082$  at the tip. In the steady state, the strong dependence of generated pore pressure magnitudes upon  $U_D$  in the region of the tip suggests that these data could be used to determine the coefficient of consolidation  $c$ , directly, since the remaining parameters in  $U_D$  are known, a priori. However, as will be discussed later, the steady magnitude of pore pressure predicted at the tip is generally the largest pore pressure magnitude observed postarrest due to consolidation effects. To determine the time required to reach steady penetration conditions the data of Fig. 2 may be normalized with respect to the ultimate steady tip pressure as represented in Fig. 3. Also included on the figure are the values of coefficient of consolidation that correspond to the appropriate  $U_D$  magnitude for a standard

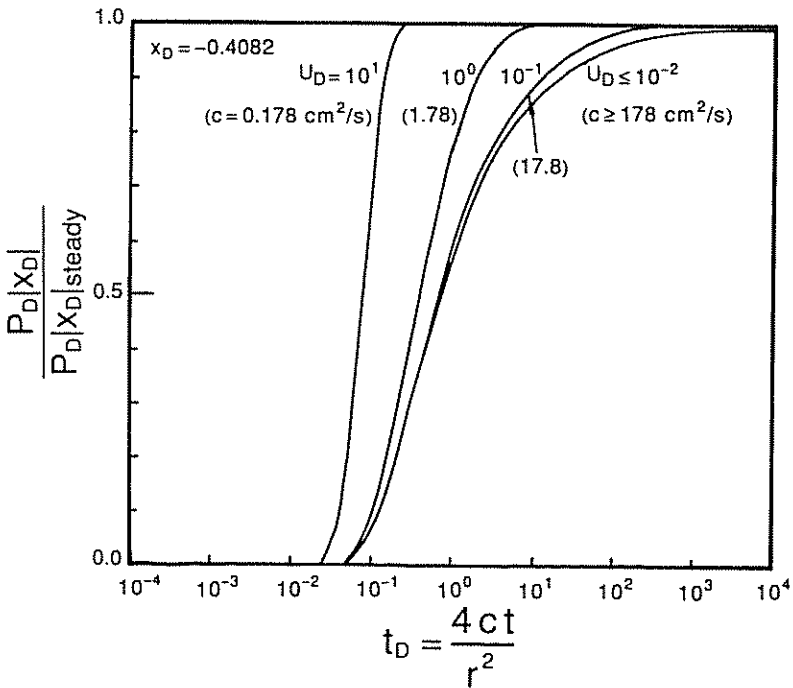


FIG. 3. Transient Generation of Normalized Pore Pressures at Tip of Standard Penetrometer

penetration rate of  $U = 2$  cm/s. As  $c$  decreases, the equilibration time is reduced in dimensionless time. Results are not plotted for  $U_D > 10^1$  since the magnitudes of  $P_D|x_D|$  are too small to accurately gauge the response.

Along the shaft, pressure buildup is controlled uniquely by the dimensionless parameters  $t_D/x_D^2$ ,  $P_D|x_D|$  and  $U_D|x_D|$  where

$$t_D = \frac{4ct}{r^2} \dots\dots\dots (6)$$

and  $t$  = time. Consequently, a single figure will suffice for all locations along the shaft. Fig. 4 illustrates that the transient behavior at any location on the shaft is similar, in form, to pressure buildup at the tip except that the magnitudes of steady pressures vary as  $1/x_D$ .

To view pressure buildup in real time it is convenient to define  $t_{95}$  as the time required to reach 95% of the steady pressure magnitude. For both tip pressures and those measured on the shaft at a separation of 10 radii behind the tip, the results may be developed in the dimensionless space  $t_D/x_D^2$  versus  $U_D|x_D|$  to illustrate the asymptotic trends at large and small  $U_D|x_D|$  in Fig. 5. The limiting values are

$$\frac{t_D}{x_D^2} = \frac{2}{U_D|x_D|} \quad \text{for } U_D|x_D| > 10^1 \dots\dots\dots (7)$$

$$\frac{t_D}{x_D^2} = 550 \quad \text{for } U_D|x_D| < 10^{-3} \text{ on shaft} \dots\dots\dots (8)$$

$$\frac{t_D}{x_D^2} = 336 \quad \text{for } U_D|x_D| < 10^{-3} \text{ at tip} \dots\dots\dots (9)$$

For a standard penetrometer,  $t_{95}$  is a unique function of  $c$  for any single

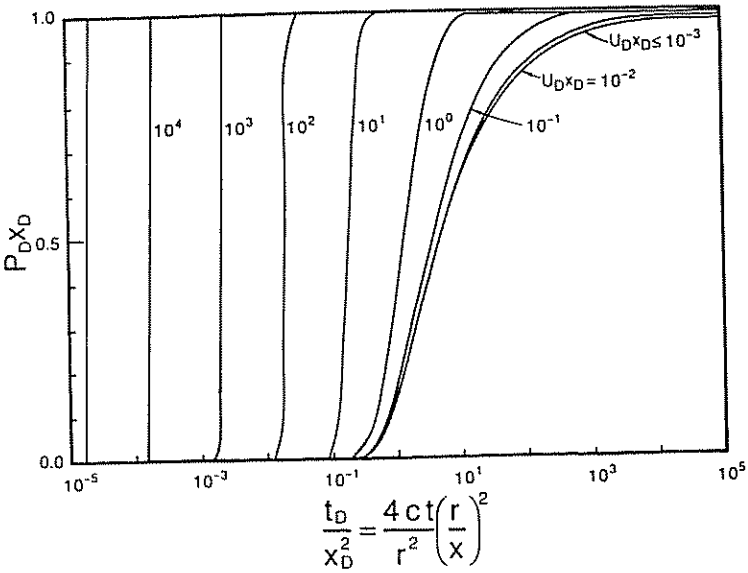


FIG. 4. Transient Generation of Dimensionless Pore Pressures along Shaft of Advancing Penetrometer

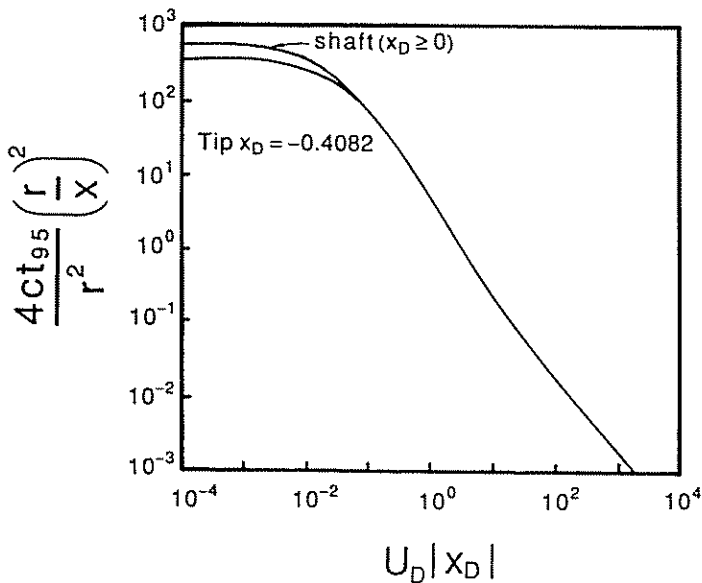


FIG. 5. Time to Reach 95% ( $t_{95}$ ) of Steady, Penetration Generated, Pore Pressure for Monitoring Locations at Tip and on Shaft

prescribed penetration rate and constant monitoring location on the instrument. This relationship is illustrated for penetration rates of  $U = 0.2, 2$  and  $20$  cm/s in Fig. 6. For penetration at a standard rate of  $2$  cm/s, shaft pressures within  $10$  radii of the tip equilibrate within  $10$  s of the initiation of drivage for  $c \leq 10$  cm<sup>2</sup>/s. A maximum equilibration time of  $35$  s is evident for  $c = 110$  cm<sup>2</sup>/s, beyond which response time asymptotically reduces. At the tip and for a standard penetration rate of  $U = 2$  cm/s, the equilibration time for  $c < 10^{-2}$  cm<sup>2</sup>/s is  $0.4$  s with a maximum possible time lag of  $1.4$  s existing for  $c = 5$  cm<sup>2</sup>/s. With reduced penetration rates, the time required to reach  $t_{95}$  is increased by an order of magnitude for each order of magnitude decrease in penetration rate except for larger values of  $c$ . As penetration rate increases, the response time is correspondingly reduced. This behavior follows directly from the time taken for any monitoring location to reach the location of the initial disturbance. Where  $c$  is small, the hydraulic disturbance will progress at a much slower rate than the moving penetrometer. As  $c$  increases, the pressure pulse moves more rapidly, relative to the penetrometer, and the time to the steady condition is controlled by the hydraulic diffusivity of the medium alone. These results suggest that dissipation tests, requiring that steady pressure distributions have been attained prior to arrest, may reasonably be conducted in a broad range of soil media providing penetration durations of the aforementioned order precede arrest.

### Steady Pressure Regime

The magnitude of tip and shaft pressures generated through the penetration process may be evaluated directly from (1) and (2). The singularity, and resulting pressure discontinuity, that exists in the vicinity of the advancing tip results in the presence of high pressure gradients. The severity

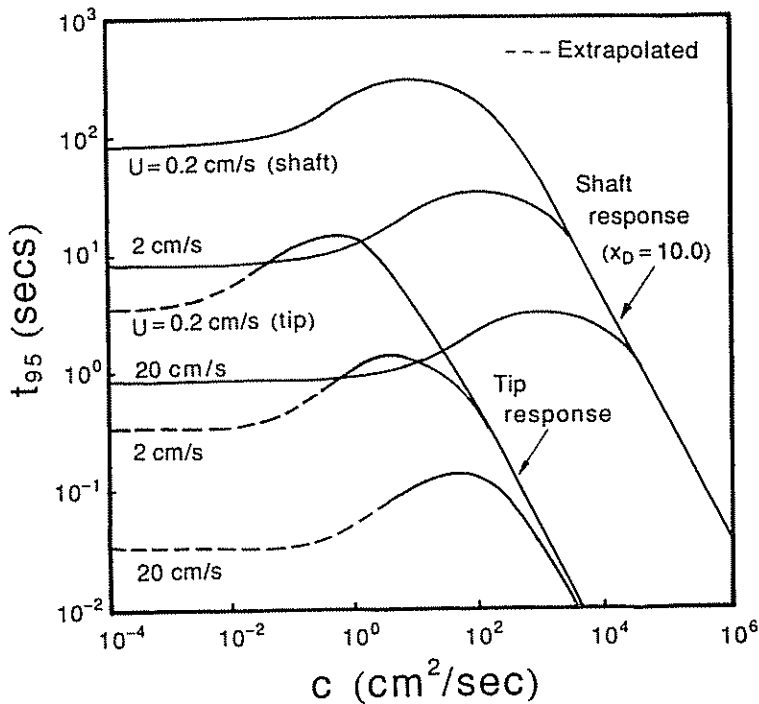


FIG. 6. Time to Reach 95% ( $t_{95}$ ) of Steady, Penetration Generated, Pore Pressure for Monitoring Locations at Tip ( $x_D = -0.4082$ ) and on Shaft ( $x_D = 10.0$ )

of these gradients increases with an increase in  $U_D$  or, under constant penetration rate, a decrease in the magnitude of  $c$ . However, following penetrometer arrest, and the resulting cessation of pore pressure generation, the severe pressure gradients present within the steady case diminish as the dissipation and pressure redistribution processes proceed. Under the control of this mechanism, pressures at the tip increase beyond the steady magnitude immediately following penetration arrest. The severity of this process is illustrated in Fig. 7, where maximum (postarrest) pressures are evidently much greater than the steady pressures for  $c < 1 \text{ cm}^2/\text{s}$ . Since dimensionless pressure is an implicit function of permeability, this relationship may be used to advantage in determining in situ permeability profiles from cone-dissipation data.

#### Transient Pressure Dissipation—Shaft

The dislocation analysis suggests that considerable ambiguity exists in the determination of consolidation parameters from postarrest dissipation histories recorded in positions along the shaft. Fig. 8 represents a generalized dissipation response for all shaft locations that exist close to a steady state immediately prior to cone arrest where  $t - t' =$  the elapsed time following penetration arrest, and  $t_D - t'_D =$  the dimensionless equivalent of (6). For soundings undertaken at a fixed penetration rate,  $U$ , the individual curves, displaced laterally in dimensionless time, represent responses for different magnitudes of coefficient of consolidation  $c$ . Since the coefficient of con-

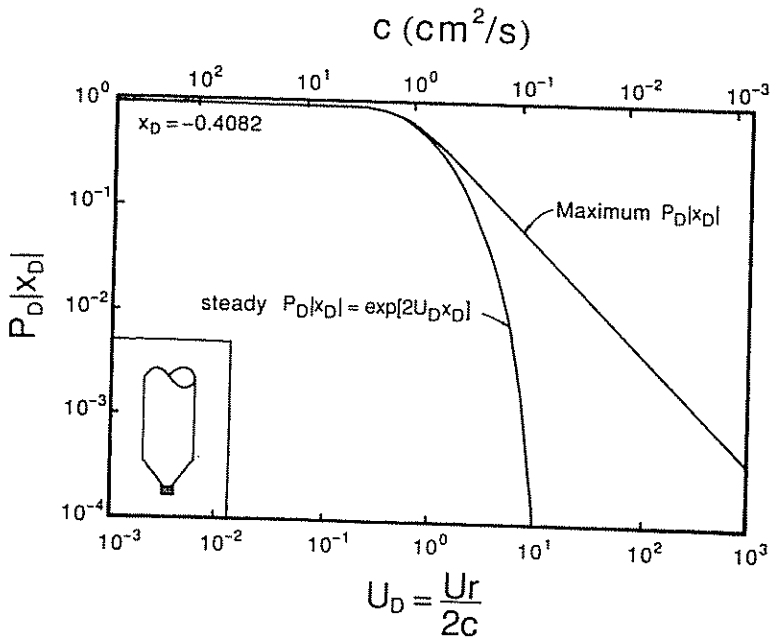


FIG. 7. Magnitudes of Steady and Maximum (Postarrest) Dimensionless Pressures Recorded at Tip of Standard Cone; Dimensional Results (for  $c$ ) Assume Steady Penetration Rate of 2 cm/s

solidation  $c$  is also an intrinsic parameter within the dimensionless time scale, it is not possible to evaluate  $c$  from shaft-dissipation results alone.

For values of dimensionless penetration rate,  $U_D$ , greater than about  $10^{-1}$  the time to 50% pressure dissipation following penetration arrest,  $(t_D - t'_D)_{50}$ , decreases one order of magnitude for each tenfold increase in  $U_D x_D$ . This is apparent from Fig. 8. From this, the relation

$$\frac{(t_D - t'_D)_{50}}{x_D^2} U_D x_D \approx 1 \quad \text{for } U_D x_D \geq 10^{-1} \dots \dots \dots (10)$$

may be constructed, that simplifies to

$$(t - t')_{50} \approx \frac{1}{2} \frac{x}{U} \quad \text{for } U_D x_D \geq 10^{-1} \dots \dots \dots (11)$$

This identifies the form of the decoupling between pressure dissipation adjacent to the shaft and the material parameters of the penetrated medium. This decoupling has important implications for the use of pressure dissipation data recorded on the shaft. For penetration with a cone of 10 cm<sup>2</sup> end-bearing area at a standard rate of 2 cm/s, the use of shaft pressures for predicting consolidation coefficients becomes problematic for consolidation coefficients less than about 20 cm<sup>2</sup>/s. This factor has considerable implications for shaft gathered data.

For a standard cone advanced at a constant rate of  $U = 2$  cm/s, the postarrest dissipation response at any single fixed shaft location remains

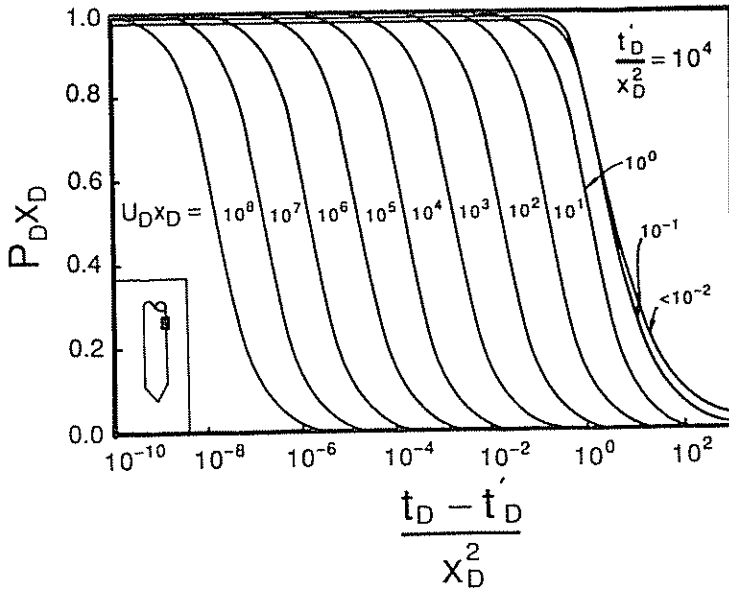


FIG. 8. Postarrest Dissipation of Pore Pressures Measured on Shaft

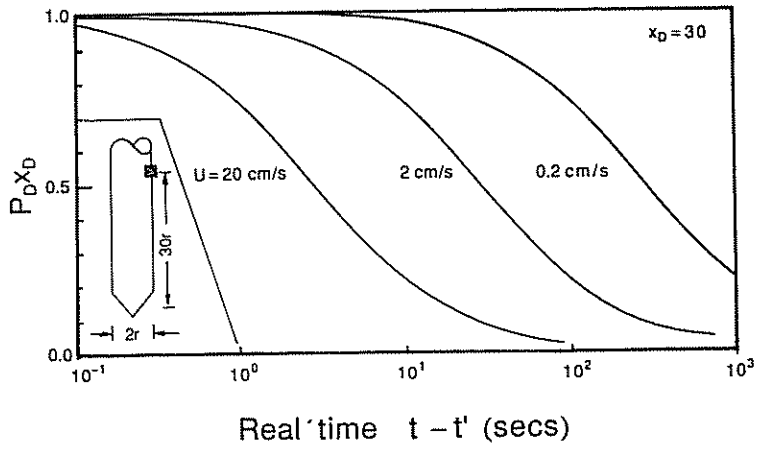


FIG. 9. Postarrest Dissipation of Shaft Pore Pressures in Real Time for Penetration Rates of  $U = 0.2, 2, \text{ and } 20 \text{ cm/s}$

uniquely constrained in real time. The candidate pressure responses at a measuring location 30 radii behind the tip are illustrated as a function of real time in Fig. 9 for penetration rates of  $U = 0.2, 2, \text{ and } 20 \text{ cm/s}$ . The dissipation response is accelerated with an increased penetration rate; however, the pressure history remains independent of the hydraulic properties of the penetrated medium. The reason for this behavior is that increased penetration rates result in an elongate distribution of induced pore pressures

conforming closely to the penetrometer shaft morphology [see, for example, Elsworth (1991)] that ultimately allows rapid pressure dissipation. The apparent decoupling of the dissipation response from the hydraulic parameters of the penetrated medium is a regrettable finding of the analysis since it directly questions the applicability of using shaft records as a basis for determining consolidation behavior in situ.

### Transient Pressure Dissipation—Tip

Pore pressures are the most commonly recorded response index and provide the greatest potential in determining consolidation behavior in situ. Postarrest pressure dissipation behavior is illustrated in Fig. 10 for the tip response of a 60° cone. For both undrained (large  $U_D$ ) and partially drained (small  $U_D$ ) behaviors the dissipation results fall within a relatively narrow band. For pressure dissipation in the vicinity of the tip, the responses are unique and may be utilized in standard type curve matching analyses. Of concern in viewing the dissipation curves for large  $U_D$  magnitudes, however, is the presence of pressure build-up following cone arrest. A dimensionless penetration rate of  $U_D = 10^2$  is equivalent to  $c = 2 \times 10^{-2}$  cm<sup>2</sup>/s under a standard, prearrest advance rate of 2 cm/s and is therefore well within the range encountered in practice. Monotonic dissipation behavior is most commonly recorded in practice although local swelling may also be evident. This particular artifact of the analysis appears more attributable to the representation of the cone tip as an infinitesimal dislocation rather than being a phenomenon that might be anticipated in reality. Because of the uncertainty engendered in determining a direct correspondence between the idealized analytical and true penetrometer geometries, it is more suitable to use maximum recorded postarrest pressure magnitudes rather than steady pressure magnitudes in later parameter determination. Steady pressure magnitudes are strongly location-dependent in the zone immediately surrounding the dilation center. Conversely, maximum pressure magnitudes reflect an aggregated response within the vicinity of the advancing tip and therefore represent global behavior more faithfully than the steady, local response.

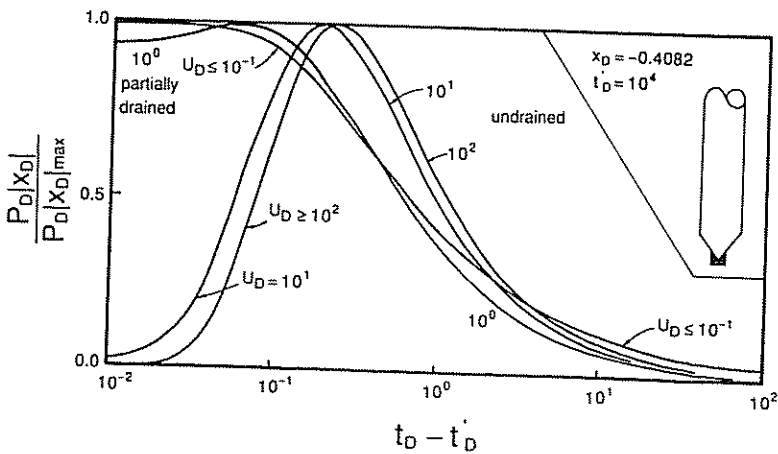


FIG. 10. Dissipation of Tip Pressures for Standard Cone; Responses are Normalized with Respect to Maximum Recorded Pressure

## RATIONAL DATA REDUCTION

As a direct consequence of the anticipated nonunique nature of pore pressure signatures measured along the penetrometer shaft, the monitoring of pressure generation and postarrest pressure dissipation responses in the region adjacent to the tip will be utilized as the only unambiguous method of determining consolidation behavior and permeability in situ.

### Coefficient of Consolidation, $c$

Monitoring of the dissipation response following cone arrest, as recognized by many others, may be used to directly evaluate the coefficient of consolidation. For a standard cone, the postarrest response is illustrated in Fig. 10. If  $t_{50}$  is defined as the time to reach 50% of the maximum, prearrest, normalized pore pressure differential, the response curves appear relatively insensitive to penetration rate. A slight steepening of the response curve is apparent as  $U_D$  increases. Following directly from Fig. 10

$$c = \frac{r^2 \alpha}{4t_{50}} \dots \dots \dots (12)$$

where

$$\alpha = 1.183 \quad \text{for } U_D \cong 10^2 \dots \dots \dots (13)$$

and

$$\alpha = 0.720 \quad \text{for } U_d \leq 10^{-2} \dots \dots \dots (14)$$

represent scaling coefficients for the limiting magnitudes of the dimensionless penetration rate  $U_D$ . It is important to note, however, that the range  $1.183 > \alpha > 0.720$  does not bound all values of  $\alpha$ , as apparent from the figure and, additionally, that the correspondence within these limits is nonlinear. Magnitudes of  $\alpha$  may be accurately recovered from Fig. 10 or, alternatively, interpolated within the relatively narrow limits set by (13) and (14) with little loss in precision.

In comparison with established methods of undrained parameter determination through dissipation tests, equivalent magnitudes of  $\alpha$  in (14) are determined as  $\alpha = 4$  by Torstensson (1977) and  $\alpha = 15.2$  by Levadoux and Baligh (1986). The variation of  $\alpha$ , in spanning more than an order of magnitude, is sobering in that the analyses purport to represent similar physical conditions. However, the recovery of correlations noting similar quantitative trends is more remarkable when viewed against the variety of behavioral and geometric assumptions incorporated within the three independent analyses. The results are particularly encouraging since the potential for extending parameter determination techniques into the partially drained regime is implicitly represented within equation (12), without modification.

### Hydraulic Conductivity, $k$

In situ permeabilities may be evaluated directly from the magnitude of the maximum postarrest pressure differential ( $\Delta u$ ) provided the coefficient of consolidation may be determined, as addressed previously. If  $c$  is known a priori, Fig. 7 documents the unique dependence upon the parameter  $P_D|x_D|$ . Two regimes are evident, approximately separated at  $U_D = 10^{-1}$ . Quoting results in terms of hydraulic conductivity  $k$  for these two regimes where  $k = \rho g c_i / \mu$  gives

$$k = \frac{5}{8} \frac{U_r \rho g}{(\Delta u)} \quad \text{for } U_D \leq 10^{-1} \dots\dots\dots (15)$$

and

$$k = \frac{1}{2} \frac{\rho g c}{(\Delta u)} \quad \text{for } U_D > 10^{-1} \dots\dots\dots (16)$$

where  $\rho$  = the density of the percolating fluid,  $g$  = gravitational acceleration,  $k_i$  = intrinsic permeability, and the maximum pressure ( $\Delta u$ ) induced at the tip is used. For standard cone geometry and a 2 cm/s penetration rate, the pressure response is dependent on the magnitude of  $c$  and known physical constants, only. For a large coefficient of consolidation (small  $U_D$ ), the magnitude of pore pressures generated adjacent to the advancing penetrometer are strongly regulated by concurrent dissipation processes in the surrounding medium and conditions of partial drainage prevail. For small  $c$  (large  $U_D$ ), the behavior is undrained and the magnitude of induced pore pressures are regulated by the elastic constants of modulus,  $E$ , and Poisson ratio,  $\nu$ , only, since the coefficient of consolidation,  $c$ , is a unique function of permeability and the elastic constants. It follows directly from (16) that the maximum pore pressure magnitudes, evident following penetration arrest, are inversely proportional to the elastic modulus. This factor highlights the desired adjunct of utilizing end bearing stresses ( $q_n$ ) in the reduction of cone data. As stiffness of the penetrated medium is increased, the traction (or stress) required to "inflate" a dislocation to a fixed volumetric magnitude is correspondingly increased. The inflation traction (or stress) directly regulates the magnitude of induced pore pressures and exercises dominant control on the pressure response at the tip under conditions of impeded drainage. End bearing stress magnitudes are important in discriminating between the pressure response signatures of materials exhibiting comparably low coefficients of consolidation but different component moduli and permeabilities.

**Cone End Bearing,  $q_n$**

As a consequence of assumptions made in the dislocation analysis, both permeabilities and coefficients of consolidation may be recovered from the pressure buildup and dissipation data. Independent evaluation of the moduli may be obtained from the end bearing resistance. The strength of the dislocation is given, by Elsworth (1991), as

$$KZ = V \frac{\mu}{k_i} c \frac{3(1 - \nu_u)}{B(1 + \nu_u)} \dots\dots\dots (17)$$

where  $KZ$  = the *strength* of the dipole triplicate required to open a cavity of volume,  $V$ , undrained Poisson ratio is  $\nu_u$ , and  $B$  = the Skempton pore pressure parameter. For an incremental advance of length  $\delta$ , then  $V = \delta \pi r^2$ , which allows the end bearing (or cavity expansion) stress  $q_n$  to be evaluated from the inflation traction,  $T$ , as

$$\frac{T}{\delta \pi r^2} = c \frac{\mu}{k_i} \frac{3(1 - \nu_u)}{B(1 + \nu_u)} = q_n \dots\dots\dots (18)$$

where the end bearing is uniquely conditioned by the elastic parameters  $E$  and  $\nu_u$ . It should be further noted that, since the dislocation is inflated within an initially unstressed medium, the magnitude of  $q_n$  is automatically corrected for the effects of overburden stress as  $q_n = q_c - \sigma_{vo}$ . Utilizing

the end bearing magnitude of (18), the pore pressure ratio  $B_q$  may also be evaluated for different dimensionless penetration rates,  $U_D$ . Utilizing (16) for  $U_D > 10^{-1}$  and substituting into (18) gives

$$B_q = \frac{(\Delta u)}{q_n} = \frac{1}{2} \frac{B(1 + \nu_u)}{3(1 - \nu_u)} = \frac{1}{2} \dots \dots \dots (19)$$

and for  $U_D < 10^{-1}$ , (15) may be substituted into (18) to give

$$B_q = \frac{(\Delta u)}{q_n} = \frac{5}{8} \frac{Ur}{c} \frac{B(1 + \nu_u)}{3(1 - \nu_u)} = \frac{5}{8} \frac{Ur}{c} \dots \dots \dots (20)$$

These results are illustrated graphically in Fig. 11. For small magnitudes of consolidation coefficient,  $B_q$  is insensitive to soil parameters as evident in (19). That the magnitude of  $B_q$ , predicted from the foregoing elastic analysis, is located firmly within the range commonly evidenced in the field, is interesting and suggests that soil stiffness plays an important role in defining pore pressure ratio. This is in addition to the influence of soil strength. As the magnitude of the coefficient of consolidation,  $c$ , increases above 4 cm<sup>2</sup>/s for standard penetration, the pore pressure ratio is reduced. This predicted behavior conforms closely with trends exhibited in cone penetrometer data and exhibits a strong correspondence with pore pressure ratio,  $B_q$ , versus cone bearing stress,  $q_n$ , correlations used routinely in qualitative stratigraphic identification [for example, Robertson et al. (1986)]. The range of consolidation coefficients,  $c$ , identified on the vertical axis also illustrate the progression from granular media, at top, to cohesive soils, at the axis base, and below.

The end bearing stress, defined in (18) may also be used to define the

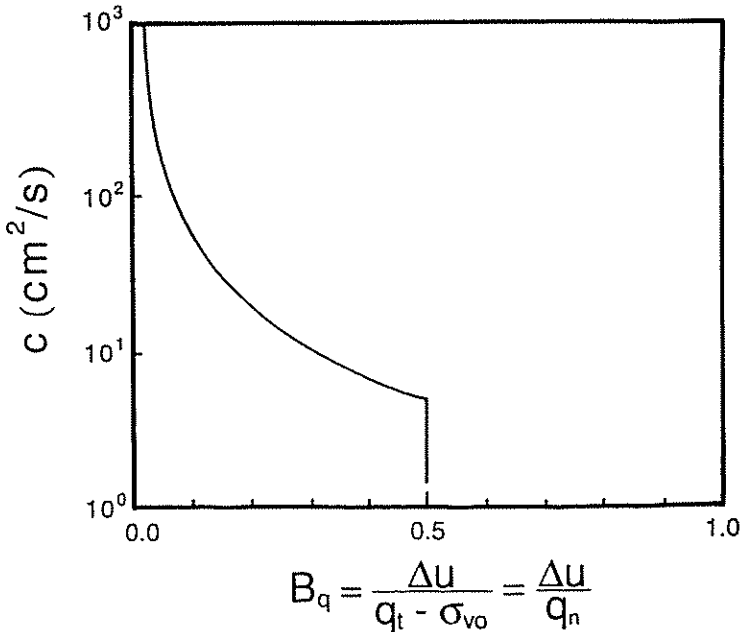


FIG. 11. Variation in Pore Pressure Ratio ( $B_q$ ) with Consolidation Coefficient ( $c$ )

modulus of the penetrated medium as identified by empirical correlations. Noting that the isotropic consolidation coefficient,  $c$ , is defined as [see Rice and Cleary (1976)]

$$c = \frac{k_i}{\mu} \frac{E(1 - \nu)}{(1 - 2\nu)(1 + \nu)} \frac{B^2(1 + \nu_u)^2(1 - 2\nu)}{9(1 - \nu_u)(\nu_u - \nu)} \dots \dots \dots (21)$$

If it is assumed that the penetrated material is sufficiently dirty that  $B = 1$  and that  $\nu_u = 0.5$ , as a first approximation, then the right-hand term of (21) reduces to unity. Under this simplification, then, substituting (21) into (18), yields

$$q_n = \frac{E(1 - \nu)}{(1 - 2\nu)(1 + \nu)} \dots \dots \dots (22)$$

or for  $\nu = 0.25$ , then  $q_n \approx 1.2E$ . This is in close agreement with empirical correlations for granular materials, such as Schmertmann (1970) where  $E = 2q_n$ . In cohesive materials, moduli are related to undrained strength,  $S_u$ , through a simple constant of proportionality, as  $E = \beta S_u$ . The proportionality coefficient,  $\beta$ , is a function of overconsolidation ratio and enables undrained shear strength to be indirectly determined from penetrometer results.

## CASE STUDIES

The parameter determination procedures, obtained directly from the dislocation analysis, are used, without modification, to determine in situ permeability and consolidation characteristics in two separate case studies. The first ("Derivation" 1987) is representative of a normally consolidated tailings deposit where partial dissipation of penetration generated pore pressures is significant, making undrained analyses inappropriate. The second suite of data (Baligh and Levadoux 1986) are for penetration in Boston Blue Clay at overconsolidation ratios of between 1.3 and 3 and represent undrained behavior at the time scale of penetration advance. These contrasting data suites examine the applicability of the dislocation model for parameter determination in normally consolidated and overconsolidated materials and under both undrained and partially drained conditions.

### Normally Consolidated Material

An extensive suite of piezocone soundings, conducted under carefully controlled conditions at an extensively documented site at Tyrone, New Mexico ("Derivation" 1987), are used. The results are complemented by a comprehensive sequence of laboratory and field testing results. The penetrometer studies are particularly unique with pressure buildup and dissipation data recorded in adjacent soundings (1.23-m separation) at advance rates spanning two orders of magnitude ( $U = 0.3, 2$  and  $20$  cm/s). The tailings deposit, to which the study pertains, comprises a normally consolidated silty clay of low plasticity, exhibiting no obvious trend of index properties ( $w_n = 20-40\%$ ,  $w_L = 27-40\%$ , plasticity index (PI) =  $5-20\%$ , liquidity index (LI) =  $0.5-1.5$ ) with depth. Natural underdrainage conditions within the soil profile reduce the static pore pressures below hydrostatic. Parameter evaluation is completed for the suite of pressure buildup and subsequent dissipation records measured, both at the tip, and along the penetrometer shaft.

*Tip Pressures*

Three separate vertical soundings are reported for penetration by a standard cone at the rates of 0.3, 2, and 20 cm/s. The three sounding locations are parallel, at a lateral separation of 1.23 m. The magnitudes of the maximum recorded pore pressures at the tip,  $\Delta u$ , and the characteristic dissipation times,  $t_{50}$ , allow consolidation coefficients and hydraulic conductivities to be evaluated directly from the test results. The static pore pressure distribution is available from long-term dissipation results and is approximately parabolic with depth, reflecting the nature of underdrainage within the tailings impoundment. Figs. 12(a)–(c) record the predicted variations of  $c$  and  $k$  with depth for penetration rates of 0.3, 2, and 20 cm/s, respectively. Also illustrated are the ranges of anticipated in situ permeabilities and consolidation coefficients (“Derivation” 1987) evaluated from static pore pressure distributions and laboratory consolidation tests. Significant

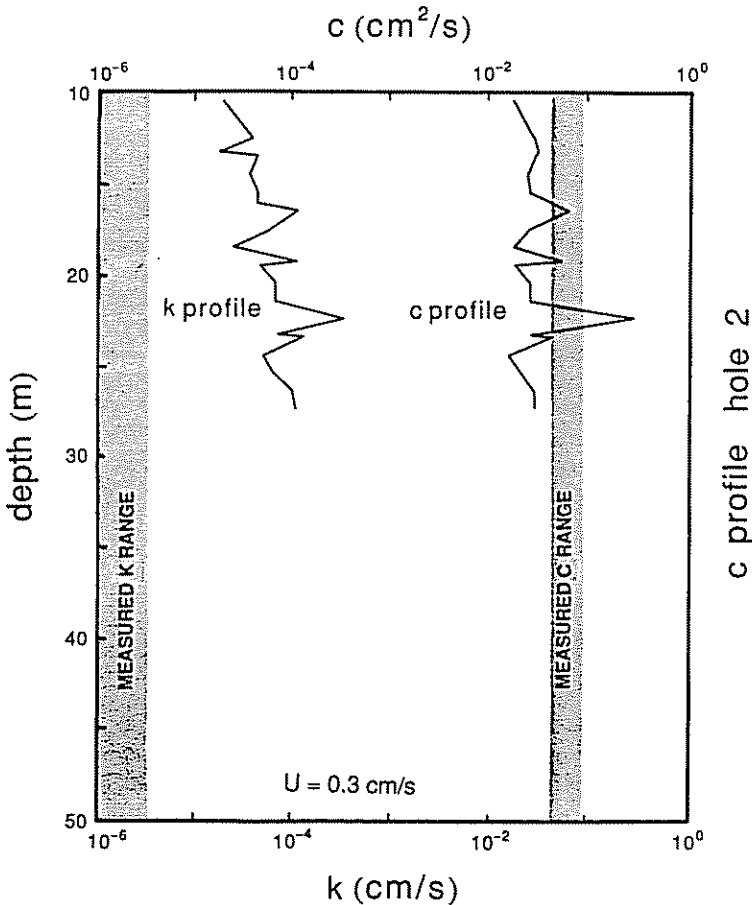


FIG. 12. Measured and Predicted Profiles of Hydraulic Conductivity ( $k$ ) and Consolidation Coefficient ( $c$ ); Soundings Completed at Penetration Rates ( $U$ ) of: (a) 0.3 cm/s; (b) 2 cm/s; and (c) 20 cm/s, at Tyrone, New Mexico

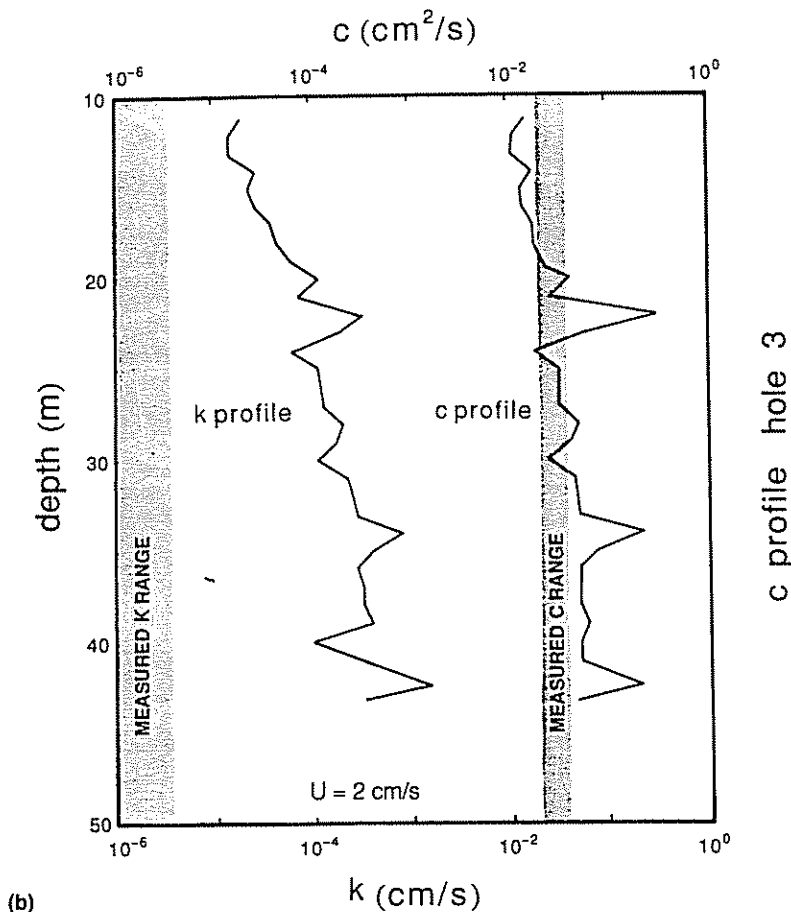
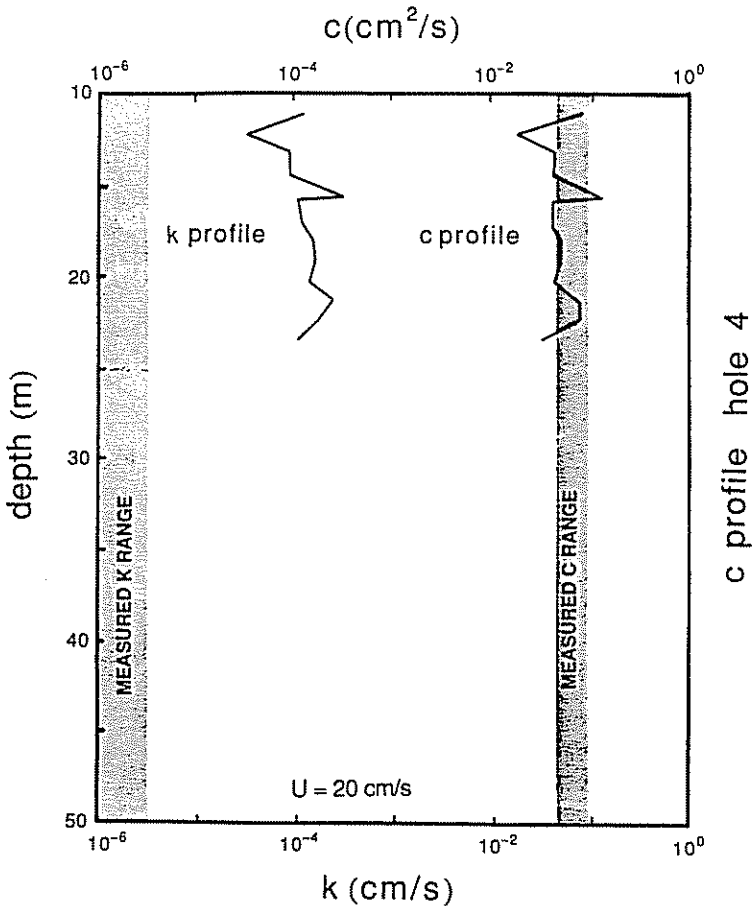


FIG. 12. (Continued)

correlation is recorded between measured and predicted magnitudes of consolidation coefficient with the correspondence between measured and predicted hydraulic conductivity magnitudes being less convincing. Most importantly, the influence of penetration rate is not apparent in the predicted coefficients of consolidation despite, the test rates spanning almost two orders of magnitude and therefore representing a spectrum of partially drained conditions. This correspondence is encouraging in determining the usefulness of the dislocation method in determining soil parameters in situ.

#### Shaft Pressures

A single sounding within the test suite recorded shaft pressures at a distance of 0.53 m (30 radii) behind the tip. Results are available for penetration rates of 0.3, 1.9, and 5.7 cm/s. Concerns over the nonuniqueness of the resulting pressure dissipation response are highlighted in Fig. 13 where dissipation histories predicted on the basis of the dislocation response are reproduced in real time together with those recorded in the field. These



(c)

FIG. 12. (Continued)

field data illustrate the predicted time shift that results from increased penetration rate, although the magnitude of the recorded shift is smaller than that predicted. Poor correspondence is evident between the predicted and measured results.

Hydraulic conductivities may be evaluated from the pressure response, since  $P_D x_D = 1.0$ , to give the profile illustrated in Fig. 14. Interestingly, the hydraulic conductivities predicted from the shaft response agree more favorably with the estimated in situ values than those derived from the reduction of the tip pressure data. However, the lack of consistency in the results, exhibited for different penetration rates, is of concern. The non-uniqueness problem, together with the apparent rate dependence of the results exhibited in Fig. 14, combine to suggest caution in the use of recorded shaft results for the determination of hydraulic material parameters in situ.

#### Pore Pressure Ratio

For the combinations of penetration rates and consolidation coefficients encountered in the testing suite, a pore pressure ratio,  $B_q$ , of 0.5 is appro-

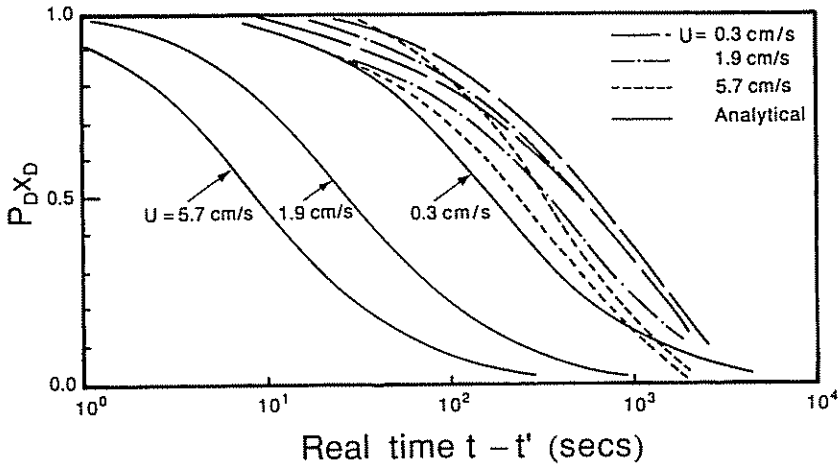


FIG. 13. Measured and Predicted Shaft Pressure Dissipation Records for Penetration Rates of  $U = 0.3, 1.9,$  and  $5.7$  cm/s; Pressures Recorded  $0.53$  m Behind Tip ( $x_D = -0.4082$ ), at Tyrone, New Mexico; Illustrated Only are Curves Bounding Dissipation Responses

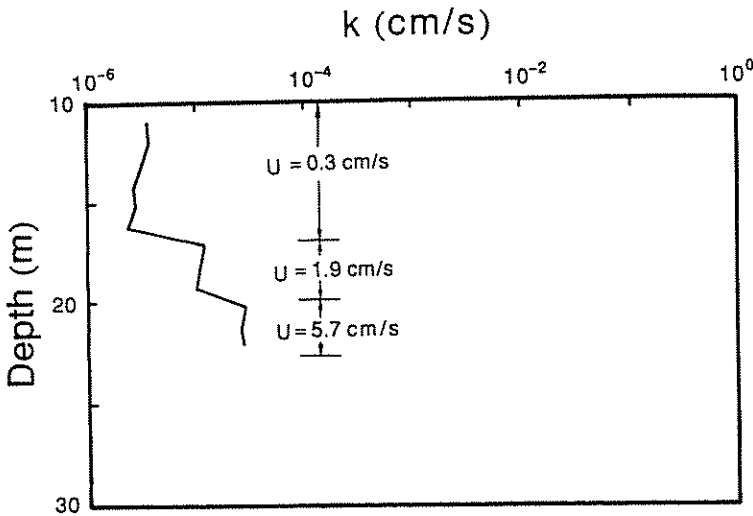


FIG. 14. Hydraulic Conductivity Profiles Obtained from Shaft Pressure Magnitudes Recorded at Tyrone, New Mexico

priate. Magnitudes of  $B_q$  recorded in the three rate-controlled soundings ranged between  $0.5-0.65, 0.4-0.8,$  and  $0.55-0.75$  for penetration rates of  $U = 0.3, 2,$  and  $20$  cm/s, respectively. No significant trend is apparent from these somewhat erratic results except to confirm the apparent independence of  $B_q$  from penetration rate [see (17)] and the insensitivity of  $B_q$  as an index parameter. Knowledge of this parameter adds no further independent information to the reduction of the test results.

## Overconsolidated Material

Data for piezocone soundings in Boston Blue Clay are reported by Baligh and Levadoux (1986) that include the measurement of undrained pore pressures developed during penetration and subsequent excess pore pressure dissipation records. In this previous work (Baligh and Levadoux 1986), the sounding records within the mildly overconsolidated material (OCR of 1.3–3) are compared with both predictions from a strain path type model and independent field and laboratory tests. To establish the applicability of the dislocation model to over consolidated materials, parameters are determined for the data derived from penetration with a 60° cone under a standard penetration rate of 2 cm/s.

### Tip Pressures

Following termination of steady penetration, dissipation rates at cone tip give time to 50% consolidation,  $t_{50}$ , in the range 300–600 s for arrest at penetration depths below 18 m [see Fig. 3 of Baligh and Levadoux (1986)]. Consolidation coefficients may be evaluated from these data using (12) and (13) and return magnitudes in the range 0.0016–0.0032 cm<sup>2</sup>/s. From this, dimensionless penetration rates are evaluated in the range  $U_D = 0.5–1.0 \times 10^3$ , confirming the choice of the calibration coefficient,  $\alpha$ , from (13). Predicted magnitudes are given in Table 1, and compare very well with consolidation coefficients in the range  $c = 0.001–0.002$  cm<sup>2</sup>/s, as determined from back analysis of excess pore pressure dissipation following embankment loading, completed by Duncan ("Proceedings" 1975). The dissipation results are for long term monitoring (7 years) of the I-95 embankment at a lateral separation of only 600 m from the sounding site. The favorable agreement is particularly encouraging.

Steady pore pressures developed during penetration are also given for arrest depths of 13.5, 18, and 25.5 m [see Fig. 1 of Baligh and Levadoux, (1986)]. Hydraulic conductivity magnitudes may also be determined from the data suite through application of (16). Using the range of consolidation coefficients ( $c = 0.001–0.002$  cm<sup>2</sup>/s) derived from the dissipation results, variations in isotropic hydraulic conductivity with penetration depth are documented in Table 1. Predicted values are in the range  $k = 1.73–4.78 \times 10^{-7}$  cm/s and compare well with laboratory measured values of  $k = 0.2–2.0 \times 10^{-7}$  cm/s [see Fig. 8 of Baligh and Levadoux (1986)].

**TABLE 1. Dislocation Method Derived Parameters from Piezocone Soundings in Boston Blue Clay (Baligh and Levadoux 1986)**

Sounding depth (m) (1)	Predicted consolidation coefficient (cm <sup>2</sup> /s) (2)	Measured consolidation coefficient <sup>a</sup> (cm <sup>2</sup> /s) (3)	Predicted hydraulic conductivity (cm/s) (4)	Measured hydraulic conductivity <sup>b</sup> (cm/s) (4)	Over-consolidation ratio (6)
13.5	(0.0016–0.0032) <sup>c</sup>	0.005	$2.46–4.78 \times 10^{-7}$	$0.4–2.0 \times 10^{-7}$	3.0
18	(0.0016–0.0032)	0.002	$1.87–3.74 \times 10^{-7}$	$0.4–1.5 \times 10^{-7}$	2.0
25.5	(0.0016–0.0032)	0.001	$1.73–3.47 \times 10^{-7}$	$0.2–1.0 \times 10^{-7}$	1.3

<sup>a</sup>Results from field matching of pore pressure response to embankment loading after Duncan ("Proceedings" 1975) and reported in Baligh and Levadoux (1986).

<sup>b</sup>Laboratory tests reported in Baligh and Levadoux (1986).

<sup>c</sup>Consolidation coefficient magnitudes assumed in predicting hydraulic conductivities.

## Shaft Pressures

Dimensionless penetration rates evaluated from pore pressure dissipation rates recorded at the tip are in the range  $U_D = 0.5-1.0 \times 10^3$ . Correspondingly, for penetration rates,  $U_D$ , greater than about  $10^{-1}$ , as identified in Fig. 8 of this work, pore pressure dissipation along the shaft is effectively decoupled from a dependence on the physical parameter of consolidation coefficient,  $c$ . This facet of the behavior is predicted directly from the dislocation method as discussed previously. Consequently, evaluation of consolidation coefficients is not attempted from this data suite.

## CONCLUSIONS

Rational methods have been presented to enable hydraulic conductivities and coefficients of consolidation to be determined directly from records of pressure buildup and subsequent dissipation obtained from cone penetrometer testing. The analysis assumes small strains and material linearity but exhibits surprising agreement in direct comparison with sounding results from well documented field sites. This is especially true for magnitudes of consolidation coefficient,  $c$ .

The results suggest that particular caution should be taken in the use of pressure buildup and dissipation responses recorded along the penetrometer shaft. The dislocation solution illustrates that for consolidation coefficients,  $c$ , less than about 20 cm/s, the dissipation response becomes decoupled from the hydraulic and displacement parameters of the medium. Dissipation rate is controlled by the parameters of prearrest penetration rate and distance of monitoring location behind the tip, alone. This is apparent in (11). This observation is contrary to the results derived from static cavity inflation theories and is an important real effect, rather than an artifact, indicated by the moving and partially drained solution, considered here. This observation is substantiated by available shaft-monitored dissipation records. This apparent problem of nonuniqueness engendered in the reduction of shaft dissipation data is especially disturbing and worthy of further field documentation.

Tip dissipation records provide a ready method for the rapid determination of coefficient of consolidation magnitudes in situ. Under undrained and partially drained conditions, alike, the simple characteristic time relationship of (12) appears effective over a full range of consolidation coefficients. For undrained results, the characteristic time relationship developed on the basis of the dislocation analysis exhibits reasonable agreement with those based upon both expanding cavity and strain path type methodologies.

The dislocation analysis allows hydraulic conductivity magnitudes to be recovered as a direct consequence of the analysis with no empirical correlations being required. The absolute magnitude of excess tip pressures are used, as defined through (15) and (16). With both  $k$  and  $c$  recovered from a single analysis, the modulus,  $E$ , is available directly, providing the magnitude of the drained Poisson ratio,  $\nu$ , is known or may be assumed. Where end bearing stresses are recorded, moduli are obtained directly from penetration records, rather than undrained strengths, as a natural artifact of the initial assumptions governing the analysis. Moduli are related to cone end bearing through a simple proportionality coefficient,  $\beta$ , as illustrated by others [e.g., (Schmertmann 1970)]. For cohesive materials, correlations of modulus with undrained shear strength may be used to determine shear strength magnitudes, indirectly.

## ACKNOWLEDGMENTS

This work is a result of partial support by the Waterloo Centre for Groundwater Research, the Natural Sciences and Engineering Research Council of Canada under Grant OGP0044021, and the U.S. National Science Foundation under grant MSM-8708976. This support is most gratefully acknowledged.

## APPENDIX I. REFERENCES

- Baligh, M. M., and Levadoux, J. N. (1986). "Consolidation after undrained piezocone penetration. II: Interpretation." *J. Geotech. Engrg. Div.*, ASCE, 112(7), 727-745.
- "Derivation and development of piezocone penetrometer data interpretation methods." (1987). *Final Report Contract No. H0245002 to the United States Bureau of Mines*, Twin Cities Research Center, Minneapolis, Minn.
- Elsworth, D. (1990). "Theory of partially drained piezometer insertion." *J. Geotech. Engrg. Div.*, ASCE, 116(6), 899-914.
- Elsworth, D. (1991). "Dislocation analysis of penetration in saturated porous media." *J. Engrg. Mech. Div.*, ASCE, 117(2), 391-408.
- Elsworth, D. (1992). "Pore pressure response due to penetration through layered media." *Int. J. Numer. Anal. Methods Geomech.*, 16(1), 45-64.
- Jones, G. A., and Van Zyl, D. J. A. (1981). "The piezometer probe—a useful investigation tool." *Proc. 10th Int. Conf. ISSMFE*, International Society for Soil Mechanics and Foundation Engineering, 2, 489-496.
- Levadoux, J. N., and Baligh, M. M. (1986). "Consolidation after undrained piezocone penetration. I: Prediction." *J. Geotech. Engrg. Div.*, ASCE, 112(7), 707-726.
- "Proceedings of the Foundation Prediction Symposium." (1975). *Research Report R80-15, Order 66*, Dept. of Civ. Engrg., Massachusetts Inst. of Tech., Cambridge, Mass., Apr.
- Rice, J. R., and Cleary, M. P. (1976). "Some basic stress diffusion solutions for fluid-saturated elastic porous media with compressible constituents." *Rev. Geophys. and Space Phys.*, 14(2), 227-241.
- Robertson, P. K., Campanella, R. G., Gillespie, D., and Greig, J. (1986). "Use of piezometer cone data." *Proc. In Situ '86, ASCE Speciality Conf. GSP 6*, ASCE, 1263-1280.
- Sanglerat, G. (1972). *The penetrometer and soil exploration*. Elsevier, New York, N.Y.
- Schmertmann, J. H. (1970). "Static cone to compute static settlement over sand." *J. Soil Mech. and Found. Div.*, ASCE, 98(3), 1011-1043.
- Skempton, A. W. (1954). "The pore pressure coefficients A and B." *Geotechnique*, 4(4), 143-147.
- Torstensson, B. A. (1977). "The pore pressure probe." *Paper No. 34*, Nordiske Geotekniske Mote, Oslo, Sweden, 34.1-34.15.
- Ylinen, A. M., and Elsworth, D. (1991). "Heat and mass transfer around an advancing penetrometer." *Int. J. Heat Mass Transfer*, 34(6), 1407-1416.

## APPENDIX II. NOTATION

*The following symbols are used in this paper:*

- $A, B$  = Skempton (1954) pore pressure coefficients;  
 $B_q$  = pore pressure ratio;  
 $c, c_h, c_v$  = coefficients of consolidation; isotropic, horizontal, vertical;  
 $E$  = modulus of elasticity;  
 $g$  = gravitational acceleration;

- $k_i, k$  = intrinsic permeability, hydraulic conductivity;  
 $l$  = cone taper length;  
 $P_D$  = dimensionless pore fluid pressure;  
 $q_c$  = cone end bearing stress;  
 $q_u$  = corrected cone end bearing stress,  $q_u = q_c - \sigma_{vo}$ ;  
 $r$  = penetrometer radius;  
 $T$  = dipole traction magnitude;  
 $t, t'$  = elapsed time, time of penetrometer arrest;  
 $t_D, t'_D$  = dimensionless elapsed time, dimensionless time of penetrometer arrest;  
 $t_{95}, t_{50}$  = time to 95% dissipation, time to 50% dissipation;  
 $U, U_D$  = penetration rate, dimensionless penetration rate;  
 $x, x_D$  = distance behind dislocation or penetrometer neutral point, dimensionless distance;  
 $\alpha$  = dissipation data calibration coefficient;  
 $\Delta u$  = induced pore pressure, or excess pore pressure;  
 $\mu$  = pore fluid dynamic viscosity;  
 $\nu, \nu_u$  = drained Poisson ratio, undrained Poisson ratio.  
 $\rho$  = pore fluid density; and  
 $\sigma_{vo}$  = initial in situ stress.

